



## Effect of refining processes on inclusions and mechanical properties of cast Al–2Li–2Cu–0.2Zr alloy

Mian RONG<sup>1</sup>, Liang ZHANG<sup>1</sup>, Guo-hua WU<sup>1</sup>, Wei-wei LI<sup>2</sup>,  
Xiao-long ZHANG<sup>1</sup>, Jiang-wei SUN<sup>1</sup>, Wen-jiang DING<sup>1</sup>

1. National Engineering Research Center of Light Alloy Net Forming and  
State Key Laboratory of Metal Matrix Composites, School of Materials Science and Engineering,  
Shanghai Jiao Tong University, Shanghai 200240, China;

2. Mag (Kunshan) New Material Technology Co., Ltd., Kunshan 215300, China

Received 26 October 2018; accepted 3 April 2019

**Abstract:** The effect of different refining processes on inclusions and mechanical properties of cast Al–2Li–2Cu–0.2Zr alloy was investigated, including two-stage hexachloroethane ( $C_2Cl_6$ ) refining process, two-stage rotating gas bubbling refining process and two-stage composite refining process. It was found that the two-stage composite refining process, which combined  $C_2Cl_6$  and rotating gas bubbling, can significantly improve the melt purity and mechanical properties of cast Al–2Li–2Cu–0.2Zr alloy. Compared to the unrefined alloy, the volume fraction of gas porosity defects and slag inclusions decreased from 1.47% to 0.12%, and the yield strength, ultimate tensile strength and elongation of as-quenched alloy increased from 113 MPa, 179 MPa and 3.9% to 142 MPa, 293 MPa and 18.1%, respectively.  $C_2Cl_6$  was first utilized to degas and remove large size slag inclusions before lithium addition, and then the rotating gas bubbling was utilized to do the further degassing and remove the suspended fine inclusions after lithium addition. The two-stage composite refining process can take advantage of two methods and get the remarkable refining effect.

**Key words:** Al–Li–Cu–Zr alloy; refining process; microstructure; melt purity; mechanical properties

### 1 Introduction

Al–Li alloys are attractive aeronautical materials and have stimulated researchers' interest in space and aerospace applications owing to their promising properties, such as very low density, high stiffness, and improved specific strength [1–5]. At present, most researches on Al–Li alloys focus on wrought alloys, while there is still lack of data on cast Al–Li alloys. This is mainly because that the wrought Al–Li alloys have the superior mechanical properties to cast alloys. The further study will focus on cast Al–Li alloys, because casting is not only a low-cost way to manufacture products with complex shapes, but also an effective method to mitigate the anisotropy of mechanical property. Moreover, the weight reduction could be much more effective in cast condition, since the limitation of lithium addition can be much higher than that in wrought alloys [6].

Due to high lithium content, the melting process of cast Al–Li alloys is extremely difficult. The affinity of lithium and hydrogen is extremely strong. The hydrogen content of molten Al–Li alloy is about 50 times higher than that of the traditional aluminum alloy without protection [7]. When the hydrogen content exceeds a certain range, the stable LiH will be formed. LiH is extremely difficult to remove, which seriously affects the melt purity and mechanical properties of cast Al–Li alloys. Moreover, lithium has extremely high chemical activity, it is easy to react with the oxygen and nitrogen during the melting process, which not only causes the burning of lithium, but also seriously affects the fluidity of the alloy melt. So the refining process is extremely important for the quality of Al–Li alloy.

In the smelting process of wrought Al–Li alloy, argon gas protection and vacuum refining are often used in order to improve the quality of continuous casting ingots. But for the cast Al–Li alloys, vacuum refining

**Foundation item:** Project (2016YFB0301003) supported by the National Key R&D Program of China; Project (51871148) supported by the National Natural Science Foundation of China; Project (sklmme-kf18-02) supported by Open Research Fund of the State Key Laboratory of Metal Matrix Composites, China

**Corresponding author:** Liang ZHANG, Tel: +86-13661663183, E-mail: liangzhang08@sjtu.edu.cn;  
Guo-hua WU, Tel: +86-13671800698, E-mail: ghwu@sjtu.edu.cn

DOI: 10.1016/S1003-6326(19)65044-2

process could not meet the needs of different casting processes (such as low-pressure casting, differential pressure casting). Therefore, it is necessary to find a suitable refining process for cast Al–Li alloys melting in normal air environment.

At present, there is a lack of research on the refining process of cast Al–Li alloys smelting under atmospheric environment. Therefore, the traditional aluminum alloy refining methods were used to refine casting Al–Li alloy.

The refining processes of traditional aluminum alloy are becoming more and more mature, including hexachloroethane ( $C_2Cl_6$ ) purifying method [8], rotating gas bubbling purifying method [9,10], ultrasonic degassing method [11,12], etc.

The conventional refining agent hexachloroethane ( $C_2Cl_6$ ) is considered the most effective refining process because of its predominant refining ability and easy operation [8,13]. However, to get the expected effects, the amount of refining agent is at least 2% (mass fraction). Large amount of hexachloroethane ( $C_2Cl_6$ ) will react in the melt to form bubbles, which will turn over on the surface of the melt. It will easily lead to gas entrainment and accelerate the oxidation of alloy elements. Moreover, using large amount of hexachloroethane ( $C_2Cl_6$ ) will result in severe environmental pollution.

As for rotating gas bubbling purifying method, it has attracted more and more attention due to its inclusion removing ability and degassing capacity [14–16]. However, neither too high or too low argon flow rate is conducive to gas and inclusions removal, and when the melt is refined overtime, the mechanical properties became poor again. Therefore, finding the reasonable parameter range of gas bubbling refining process is the key to get good refining effect.

Lots of cast Al–Li alloys have been developed and investigated in recent years. For example, Al–2Li–2Cu–0.2Zr alloy, which was studied by ZHANG et al [17,18], has good properties and can be used as a substitute for traditional high strength cast aluminum alloy. However, there is a lack of research on refining process. In this

case, effect of different refining processes on the melt purity, microstructure and related mechanical properties of Al–2Li–2Cu–0.2Zr alloy were investigated in detail. The results will promote the development and application of cast Al–Li alloys.

## 2 Experimental

Cast Al–2Li–2Cu–0.2Zr alloy used in the present study was prepared from commercially pure (CP)Al, pure Li, master alloys of Al–10%Zr and Al–50%Cu melting in an electronic resistance furnace at 770 °C under the protection of LiCl–LiF flux mixture. Four tests were set up based on different refining processes. The brief description of four processes is shown in Table 1. The flow diagram of four different refining processes is shown in Fig. 1.

**Table 1** Different refining processes applied in this work

Test No.	Refining process
I	Unrefined
II	1 wt.% $C_2Cl_6$ + 1 wt.% $C_2Cl_6$
III	Gas bubbling + gas bubbling
IV	1 wt.% $C_2Cl_6$ + gas bubbling

Test I was a blank test, neither hexachloroethane ( $C_2Cl_6$ ) or rotating gas bubbling was applied to this test. Two-stage hexachloroethane ( $C_2Cl_6$ ) refining process was used in Test II. The 1 wt.% hexachloroethane ( $C_2Cl_6$ ) was first utilized to degas at 740–750 °C before lithium addition. After adding lithium, 1 wt.% hexachloroethane ( $C_2Cl_6$ ) was utilized to degas at 730–740 °C. Then the molten metal was poured carefully into the permanent metallic mold, which was preheated at 200 °C.

Two-stage rotating gas bubbling refining process was used in Test III. The rotating gas bubbling purifying was first utilized to degas at 740–750 °C before lithium addition. After adding lithium, the rotating gas bubbling purifying was utilized to degas at 730–740 °C. The

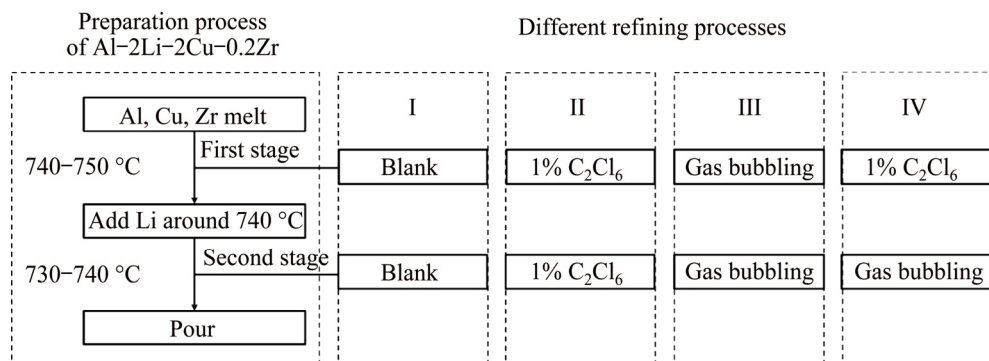


**Fig. 1** Flow diagram of different refining processes applied in this work

parameters of two bubbling processes are same: the rotating speed was 175–200 r/min, the gas flow rate was 1.5–2.0 L/min and the refining process lasted for 5–7 min. Then the molten metal was poured carefully into the permanent metallic mold, which was preheated at 200 °C. The rotating gas bubbling schematic diagram is shown in Fig. 2. The aluminum alloy was melted in a graphite crucible with a capacity of 8 kg. The graphite nozzle was 300 mm in length and 20 mm in diameter. Some of holes with a diameter of 2 mm were arranged at bottom of the nozzle. Argon passed through the hollow stainless steel pipe connected with the upper part of the nozzle and ejected from the small holes to stir the melt.

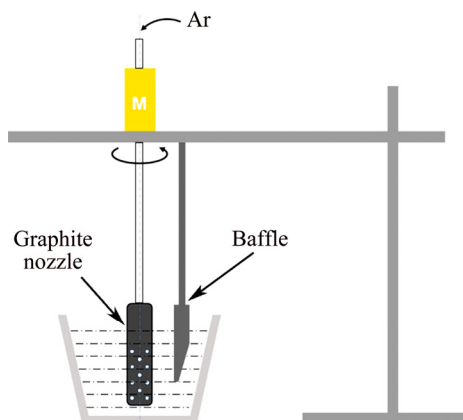


Fig. 2 Schematic diagram of rotating nozzle degasser with argon

Two-stage composite refining process which combined rotating gas bubbling and hexachloroethane ( $C_2Cl_6$ ) was used in Test IV. The 1 wt.% hexachloroethane ( $C_2Cl_6$ ) was first utilized to degas at 740–750 °C before lithium addition. After adding lithium, the rotating gas bubbling purifying was utilized to degas at 730–740 °C. The rotating speed was 175–200 r/min, the gas flow rate was 1.5–2.0 L/min and the refining process lasted for 5–7 min. Then the molten metal was poured carefully into the permanent metallic mold, which was preheated at 200 °C.

The real chemical compositions of the studied alloy, measured by inductively couple plasma-atomic emission spectroscopy (ICP-AES), are listed in Table 2. The composition of Li, Cu, Zr were similar to the design of components.

Table 2 Measured chemical compositions of Al–2Li–2Cu–0.2Zr alloys (wt.%)

Test No.	Li	Cu	Zr	Na	K	Al
I	2.03	1.84	0.22	0.051	0.0043	Bal.
II	2.14	1.79	0.17	0.050	0.0049	Bal.
III	1.97	2.12	0.16	0.048	0.0058	Bal.
IV	2.17	1.88	0.21	0.063	0.0067	Bal.

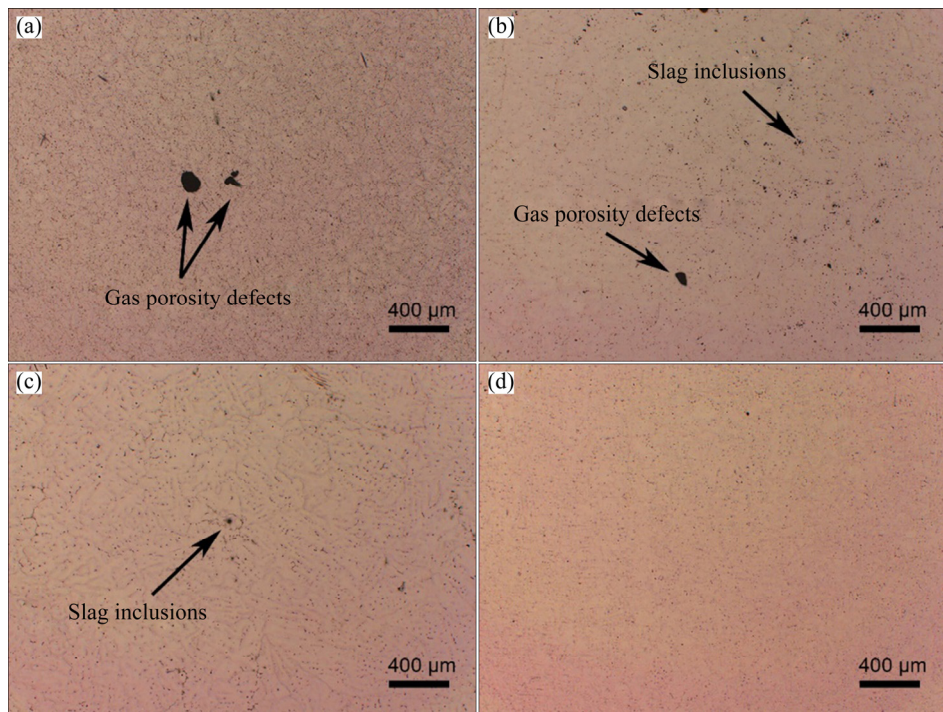
As-quenched treatment ((460 °C, 32 h) + (520 °C, 24 h)) was applied to these cast ingots. In this process, the samples were buried in sand to prevent the absence of Li on the surface. Quenching was realized in hot water at 60 °C.

The densities of alloys were measured using the standard Archimedes method with distilled water. Statistical volume fractions of nonmetallic inclusions in alloys were measured with Image-Pro Plus software. Optical samples were prepared by mechanically grounded with SiC papers to 7000 grit and polished through standard procedures. Polished specimens were etched by Keller's reagent (5 mL  $HNO_3$ , 3 mL  $HCl$ , 2 mL  $HF$  and 190 mL distilled water) for 20 s prior to characterization. The microstructure was observed using an optical microscopy (OM, LEICA MEF4M) and scanning electron microscopy (SEM, Phenom XL). Energy dispersive spectroscopy (EDS) was employed to identify the phase constitutions. The tensile properties were tested at room temperature with a cross-head speed of 1 mm/min using Zwick/ Roell Z100 tensile machine equipped with a noncontact extensometer. Sheet tensile samples of 3.5 mm in width, 2.0 mm in thickness, and 15 mm in gauge length were cut from the casting ingots by the electric-sparking wire-cutting machine. Every tensile value was determined as the average of five test results.

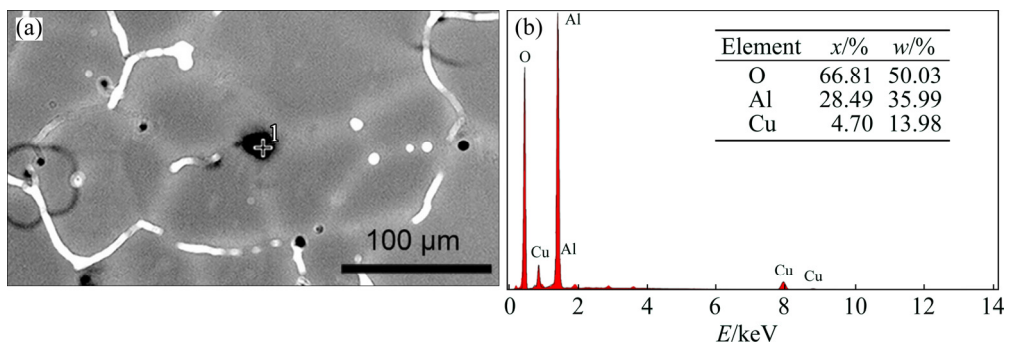
### 3 Results

Figure 3 presents the representative optical microstructures of the as-cast Al–2Li–2Cu–0.2Zr alloys refined by different refining processes. The effects of different refining processes can be reflected by the size and distribution of gas porosity defects and slag inclusions. It was clear that compared to the unrefined alloy in Fig. 3(a), the gas porosity defects and slag inclusions were reduced after hexachloroethane ( $C_2Cl_6$ ) (Fig. 3(b)) and rotating gas bubbling refining process (Fig. 3(c)), while the two-stage composite refining process which combined hexachloroethane ( $C_2Cl_6$ ) and rotating gas bubbling got the best effect, there was no obvious gas porosity defects and slag inclusions in Fig. 3(d).

Figure 4 presents the SEM image and EDS analysis of slag inclusions of unrefined alloy. The EDS point analysis was conducted to clarify the composition of slag inclusions. Element Cu is significantly enriched at the grain boundaries because its distribution coefficient [19], so the Cu also tends to be enriched at the boundaries of slag inclusions and then can be detected at point 1. Element Li has high chemical activity, it tends to oxidize rapidly and is easy to form oxidized inclusions during the melting process. Moreover, the hydrogen content of



**Fig. 3** Microstructures of as-cast Al-2Li-2Cu-0.2Zr alloy after different refining processes: (a) Unrefined; (b) 1 wt.%  $C_2Cl_6$  + 1 wt.%  $C_2Cl_6$ ; (c) Gas bubbling + Gas bubbling; (d) 1 wt.%  $C_2Cl_6$  + Gas bubbling



**Fig. 4** SEM image (a) and EDS result of point 1(b) of slag inclusions in unrefined alloy

unrefined alloy is high. When the hydrogen content exceeds a certain range, LiH will be formed. But element Li and H can not be detected under EDS. In conclusion, the chemical composition of inclusion shown in Fig. 4(b) was not accurate, the main composition of slag inclusions should be LiH and oxides of Al and Li [20].

Table 3 shows the statistical volume fractions of gas porosity defects and slag inclusions in alloys. Compared with the unrefined alloy, it was obvious that the other three refining processes significantly reduced the gas porosity defects and slag inclusions. It should be noted that the volume fraction of gas porosity defects and slag inclusions for two-stage composite refining process was 0.12 vol.%, and it was lower than that refined by the conventional 2 wt.%  $C_2Cl_6$  (0.87 vol.%). The result indicated that the application of the rotating gas bubbling can substantially improve the efficiency of  $C_2Cl_6$  refining by decreasing the amount of  $C_2Cl_6$  at a rate of 50%.

**Table 3** Statistical volume fractions of gas porosity defects and slag in alloys

Refining process	Number of fields	Average volume fraction/%
Unrefined	30	1.47
1 wt.% $C_2Cl_6$ + 1 wt.% $C_2Cl_6$	30	0.87
Gas bubbling + gas bubbling	30	0.42
1 wt.% $C_2Cl_6$ + gas bubbling	30	0.12

Table 4 shows the densities of the alloys refined by four different refining processes. The density of unrefined alloy was  $2.46\text{ g}/\text{cm}^3$ , much lower than others. This was actually due to the large amount of gas porosity defects and slag inclusions in unrefined alloy. In general, the contents of gas porosity defects and slag inclusions were inversely proportional to the alloy densities.

**Table 4** Densities of alloys refined by different processes

Refining process	Density/(g·cm <sup>-3</sup> )
Unrefined	2.46
1 wt.% C <sub>2</sub> Cl <sub>6</sub> + 1 wt.% C <sub>2</sub> Cl <sub>6</sub>	2.54
Gas bubbling + gas bubbling	2.53
1 wt.% C <sub>2</sub> Cl <sub>6</sub> + gas bubbling	2.59

The mechanical properties of the alloys refined by different refining processes are illustrated in Fig. 5. Results indicated that the mechanical properties were significantly improved after refining process. Generally,

two-stage composite refining process got the best result. The YS and UTS reached at 142 MP and 293 MP, which were 26% and 64% higher than unrefined one. The elongation got the most obvious increase and reached at 18.1%, which was 364% higher than unrefined one. This was mainly because the refining process makes the gas porosity defects and slag inclusions in alloy reduce significantly, and improve the mechanical properties (see Fig. 5(b)).

Figure 6 presents the fracture surface SEM micrographs of the tensile specimens of the Al–2Li–2Cu–0.2Zr alloys refined by different refining processes.

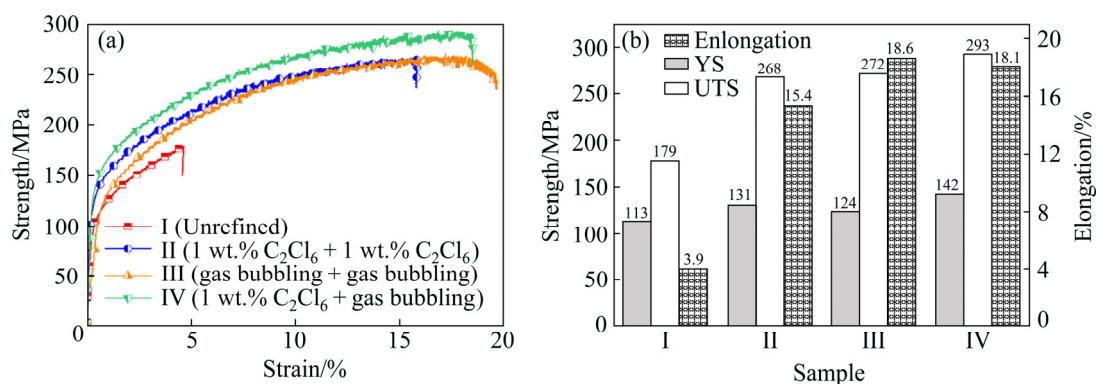


**Fig. 5** Strength–strain curves (a) and tensile properties (b) of as-quenched Al–2Li–2Cu–0.2Zr alloy after different refining processes

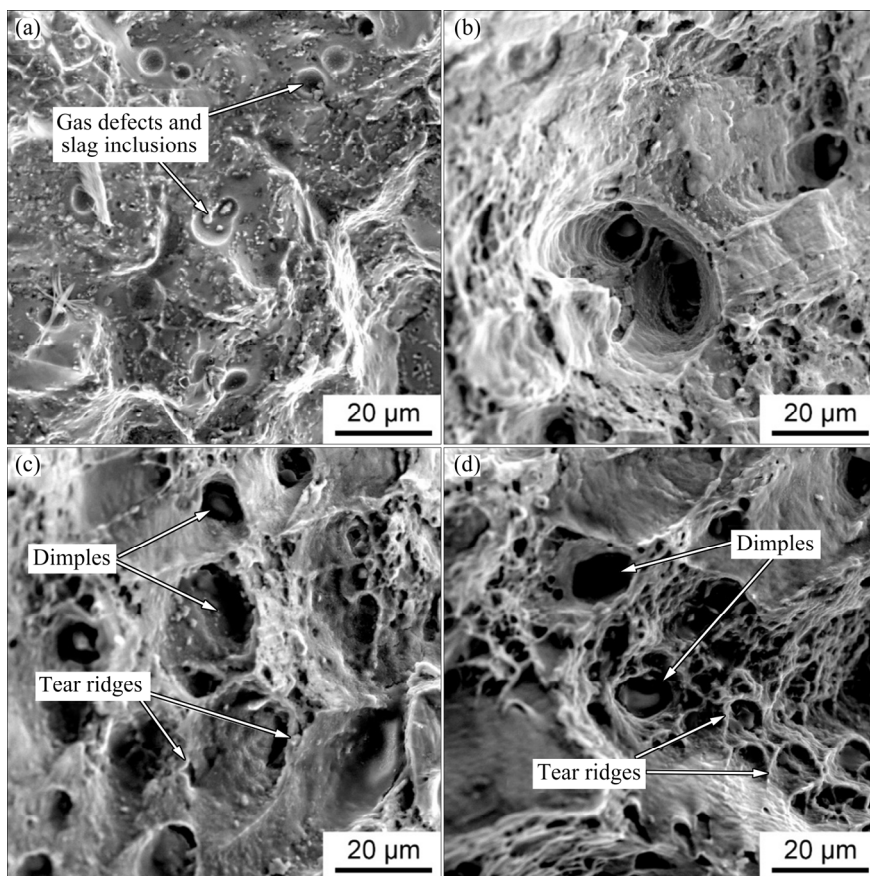


**Fig. 6** SEM fractographs showing tensile fracture surfaces of Al–2Li–2Cu–0.2Zr alloy after different refining processes: (a) Unrefined; (b) 1 wt.% C<sub>2</sub>Cl<sub>6</sub> + 1 wt.% C<sub>2</sub>Cl<sub>6</sub>; (c) Gas bubbling + gas bubbling; (d) 1 wt.% C<sub>2</sub>Cl<sub>6</sub> + gas bubbling

In unrefined alloy (see Fig. 6(a)), some gas porosity defects and slag inclusions were found on the fracture surface which indicated that the micro-crack may apart from them and then progress across the grains as cleavage fracture [21]. As demonstrated in Figs. 6(b–d), it was obvious that all of the as-quenched specimens typically demonstrated ductile fracture mode, with large amounts of isometric dimples [22]. For the alloy refined by rotating gas bubbling process and two-stage composite refining process, cleavage planes were weaker and evident isometric dimples and tearing ridges on the alloy fracture surfaces were observed (see Figs. 6(c, d)). It also explained that the specimens after refining processes III and IV got better plasticity improvement because of more dimples and tearing ridges, which was in accordance with the tensile test results.

## 4 Discussion

The principle of degassing and slag inclusions removal of hexachloroethane ( $C_2Cl_6$ ) and rotating gas bubbling method are similar. A large number of bubbles absorb gas and slag inclusions during the floating process to achieve refining purposes. The difference is that the bubbles in rotating gas bubbling method are formed by blowing argon through the nozzle, and the bubbles in  $C_2Cl_6$  method are formed by the reaction of  $C_2Cl_6$  in aluminum melt.

The reactions of  $C_2Cl_6$  in aluminum melt are generally as follows [23]:



Among these reaction products,  $Cl_2$ ,  $C_2Cl_4$ ,  $AlCl_3$  and  $HCl$  are all gaseous state at high temperatures, and all of them can form bubbles to adsorb gas and slag inclusions like argon.  $Cl_2$  can also react with  $[H]$  in aluminum melt, and achieve the hydrogen removal to some degree.

Figure 7 shows the refining principle of rotating gas bubbling method [24]. The inclusions can be wetted by the argon gas, and then float up. The particle settling velocity can be illustrated as

$$v = \frac{2g}{9\eta_{\text{metal}}r} [r_{\text{inclusion}}^3 (\rho_{\text{inclusion}} - \rho_{\text{gas}}) + r^3 (\rho_{\text{gas}} - \rho_{\text{metal}})] \quad (5)$$

where  $g$  is the gravity acceleration;  $\eta_{\text{metal}}$  is the viscosity coefficient;  $r_{\text{inclusion}}$  is the inclusion particle radius;  $r$  is the radius of aggregate of inclusion absorbing gas;  $\rho_{\text{inclusion}}$  is the inclusion density;  $\rho_{\text{gas}}$  is the gas density;

$\rho_{\text{metal}}$  is the metal density.

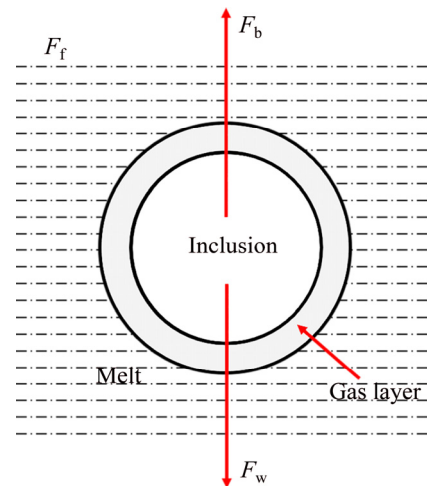


Fig. 7 Schematic diagram of inclusion particle with gas covered

Unrefined alloy has a high internal hydrogen content. When the hydrogen content exceeds a certain range,  $LiH$  will be formed. And the elements  $Al$  and  $Li$  are easily oxidized under the unrefined condition. In conclusion, the main composition of slag inclusions should be  $LiH$  and oxides of  $Al$  and  $Li$ .

As for the alloy refined by rotating gas bubbling method, the hydrogen content of the alloy is reduced, so  $LiH$  will not be formed. However, during this refining process, the generation of oxidized slag is inevitable, so the main composition of slag inclusions should be oxides of  $Al$  and  $Li$ .

As for the slag inclusions in alloy refined by refining agent ( $C_2Cl_6$ ), the composition can be inferred by following chemical reaction:



At high temperatures (700–800 °C), the pyrolysis of  $C_2Cl_6$  produced  $Cl_2$  (see Reaction (1)),  $Cl_2$  reacted with  $Li$  in the melt and formed  $LiCl$ , which did not decompose at high temperatures. Therefore, the main components of slag inclusions should be  $LiCl$  and some of the oxides of  $Al$  and  $Li$ .

In the melting process of cast  $Al$ – $Li$  alloy, the melting process of  $Li$  is the most important step. Owing to the high chemical activity of  $Li$ , it tends to oxidize rapidly and burn in air to bring a lot of inclusions into the aluminum melt during the melting process. Therefore, the first stage refining is necessary before adding  $Li$  to ensure the purity of the melt. Then, after the lithium is melted, the second stage refining is carried out to reduce the oxidation of lithium and remove the gas porosity defects and slag inclusions in the melt.

The new two-stage composite refining process which combined hexachloroethane ( $C_2Cl_6$ ) and rotating

gas bubbling got the best effect. The basic reason is that the state of melt is different before and after adding Li. Before adding Li, the gas content and slag inclusions content in the melt are large. In order to obtain a better refining effect, the flow rate of argon gas must be large enough, which inevitably leads to the tumbling of the melt surface and the possibility of air entrapment and oxidation of alloying elements. The rotating gas bubbling treatment cannot remove them effectively with low flow rate of argon, while hexachloroethane ( $C_2Cl_6$ ) can do it better. Therefore, the use of hexachloroethane ( $C_2Cl_6$ ) before adding Li can effectively remove most of the gas and large-size slag inclusions in the melt. After adding Li, the melt is easy to oxidize extremely. Therefore, ensuring the stable surface of the melt and preventing oxidation of Li are the key points of refining. The pyrolysis of  $C_2Cl_6$  produced  $Cl_2$ ,  $Cl_2$  reacted with Li in the melt and formed  $LiCl$ . Moreover,  $C_2Cl_6$  also produces a large number of bubbles, and the bubbles will turn over on the surface of the melt, which will easily lead to gas entrainment and accelerate the oxidation of Li. After the first stage refining, the remainder slag inclusions in the melt are small, which can be effectively removed by rotating gas bubbling method with low flow rate. The rotating speed and gas flow rate can be adjusted to a reasonable range (175–200 r/min and 1.5–2.0 L/min) to ensure the melt surface stable. Furthermore, Li is difficult to oxidize under argon atmosphere. The rotating gas bubbling method is the best choice to remove the gas and slag inclusions after adding Li. Therefore, the new two-stage composite refining process which combined hexachloroethane ( $C_2Cl_6$ ) and rotating gas bubbling method is the most suitable refining process for cast Al–Li alloys.

## 5 Conclusions

(1) The main composition of slag inclusions in unrefined alloy should be  $LiH$  and oxides of Al and Li.  $LiCl$  will be formed as a new kind of slag inclusion when the alloy is refined by hexachloroethane ( $C_2Cl_6$ ) after Li addition.

(2) The new two-stage composite refining process which combined  $C_2Cl_6$  and rotating gas bubbling was developed as an effective refining process for the cast Al–2Li–2Cu–0.2Zr alloy. Compared to the unrefined alloy, the YS, UTS and elongation of as-quenched alloy increased from 113 MPa, 179 MPa and 3.9% to 142 MPa, 293 MPa and 18.1%, respectively.

(3) The use of  $C_2Cl_6$  can effectively remove most of the gas and large-size slag inclusions in the melt before Li addition. The rotating gas bubbling process can remove the remainder small slag inclusions with low flow rate after Li addition. Compared to the unrefined

alloy, the volume fraction of gas porosity defects and slag inclusions decreased from 1.47% to 0.12%. The new two-stage composite refining process is the suitable refining process for cast Al–2Li–2Cu–0.2Zr alloy in this work.

## References

- [1] DURSUN T, SOUTIS C. Recent developments in advanced aircraft aluminium alloys [J]. Materials & Design, 2014, 56: 862–871.
- [2] GĄSIOR W, DĘBSKI A, TERLICKA S. Calorimetric and electromotive force measurements of Al–Li–Zn liquid solutions [J]. Journal of Phase Equilibria & Diffusion, 2016, 15: 1–10.
- [3] DENG Y L, YANG J L, SI-YU L I, ZHANG J, ZHANG X M. Influence of Li addition on mechanical property and aging precipitation behavior of Al–3.5Cu–1.5Mg alloy [J]. Transactions of Nonferrous Metals Society of China, 2014, 24: 1653–1658.
- [4] LI Hong-ying, SU Xiong-jie, YIN Hao, HUANG De-sheng. Microstructural evolution during homogenization of Al–Cu–Li–Mn–Zr–Ti alloy [J]. Transactions of Nonferrous Metals Society of China, 2013, 23(9): 2543–2550.
- [5] LI Jin-feng, LIU Ping-li, CHEN Yong-lai, ZHANG Xu-hu, ZHENG Zi-qiao. Microstructure and mechanical properties of Mg, Ag and Zn multi-microalloyed Al–(3.2–3.8)Cu–(1.0–1.4)Li alloys [J]. Transactions of Nonferrous Metals Society of China, 2015, 25(7): 2103–2112.
- [6] CHEN A, PENG Y, ZHANG L, WU G, LI Y. Microstructural evolution and mechanical properties of cast Al–3Li–1.5Cu–0.2Zr alloy during heat treatment [J]. Materials Characterization, 2016, 114: 234–242.
- [7] ZOU C L, GENG G H, CHEN W Y. Development and application of aluminium-lithium alloy [J]. Applied Mechanics and Materials, 2014, 599–601: 12–17.
- [8] WESTBERG H B, SELD N A I, BELLANDER T. Emissions of some organochlorine compounds in experimental aluminum degassing with hexachloroethane [J]. Applied Occupational and Environmental Hygiene, 1997, 12: 178–183.
- [9] WU R, QU Z K, SUN B, SHU D. Effects of spray degassing parameters on hydrogen content and properties of commercial purity aluminum [J]. Materials Science & Engineering A, 2007, 456: 386–390.
- [10] ZHAO L, PAN Y, LIAO H, WANG Q. Degassing of aluminum alloys during re-melting [J]. Materials Letters, 2012, 66: 328–331.
- [11] ESKIN G I. Cavitation mechanism of ultrasonic melt degassing [J]. Ultrasonics Sonochemistry, 1995, 2(S): s137–s141.
- [12] PUGA H, BARBOSA J, GABRIEL J, SEABRA E, RIBEIRO S, PROKIC M. Evaluation of ultrasonic aluminium degassing by piezoelectric sensor [J]. Journal of Materials Processing Technology, 2011, 211: 1026–1033.
- [13] HÅKAN B. WESTBERG, ANDERS I. SELDÉN, BELLANDER T. Emissions of some organochlorine compounds in experimental aluminum degassing with hexachloroethane [J]. Applied Occupational & Environmental Hygiene, 1997, 12(3): 178–183.
- [14] SUN Hui, MO Xiao-fei, ZHENG Rui-xiang. Numerical investigations of rotating spray degassing processing for aluminum melt [J]. Materials Science & Technology, 2010, 18: 619–623.
- [15] LEROY C, PIGNAULT G. The use of rotating-impeller gas injection in aluminum processing [J]. Journal of Metals, 1991, 43: 27–30.
- [16] ANZA I, MAKHLOUF M M. Synthesis of aluminum-titanium carbide micro and nanocomposites by the rotating impeller in-situ gas–liquid reaction method [J]. Metallurgical & Materials Transactions B, 2018, 49(1): 466–480.

[17] ZHANG X, ZHANG L, WU G, SHI C, ZHANG J. Influences of Mg content on the microstructures and mechanical properties of cast Al–2Li–2Cu–0.2Zr alloy [J]. Journal of Materials Science, 2019, 54: 791–811.

[18] ZHANG X, ZHANG L, WU G, LIU W, SHI C, TAO J, SUN J. Microstructural evolution and mechanical properties of cast Al–2Li–2Cu–0.5Mg–0.2Zr alloy during heat treatment [J]. Materials Characterization, 2017, 132: 312–319.

[19] SHI C, ZHANG L, WU G, ZHANG X, CHEN A, TAO J. Effects of Sc addition on the microstructure and mechanical properties of cast Al–3Li–1.5Cu–0.15Zr alloy [J]. Materials Science & Engineering A, 2016.

[20] PRASAD N E, GOKHALE A A, WANHILL R J H. Aluminum–lithium alloys: Processing, properties, and applications [M]. Butterworth-Heinemann, 2013.

[21] ZHANG H, FAN J, ZHANG L, WU G, LIU W, CUI W, FENG S. Effect of heat treatment on microstructure, mechanical properties and fracture behaviors of sand-cast Mg–4Y–3Nd–1Gd–0.2Zn–0.5Zr alloy [J]. Materials Science & Engineering A, 2016, 677: 411–420.

[22] FENG S, LIU W, ZHAO J, WU G, ZHANG H, DING W. Effect of extrusion ratio on microstructure and mechanical properties of Mg–8Li–3Al–2Zn–0.5Y alloy with duplex structure [J]. Materials Science & Engineering A, 2017, 692: 9–16.

[23] WHITE M L, KUNTZ R R. The pyrolysis of hexachloroethane [J]. International Journal of Chemical Kinetics, 1973, 5: 295–299.

[24] MEI Jun, LIU Wen-cai, WU Guo-hua, ZHANG Yang, ZHANG Yi-tao, HONG Yi-kai, ZHANG Ruo-xi, XIAO Lü, DING Wen-jiang. Effect of complex melt-refining treatment on microstructure and mechanical properties of sand-cast Mg–10Gd–3Y–0.5Zr alloy [J]. Transactions of Nonferrous Metals Society of China, 2015, 25: 1811–1821.

## 精炼工艺对铸造 Al–2Li–2Cu–0.2Zr 合金 夹杂物和力学性能的影响

荣冕<sup>1</sup>, 张亮<sup>1</sup>, 吴国华<sup>1</sup>, 李炜炜<sup>2</sup>, 张小龙<sup>1</sup>, 孙江伟<sup>1</sup>, 丁文江<sup>1</sup>

1. 上海交通大学 材料科学与工程学院 轻合金精密成型国家工程研究中心

金属基复合材料国家重点实验室, 上海 200240;

2. 鼎镁(昆山)新材料科技有限公司, 昆山 215300

**摘要:** 研究不同精炼工艺对铸造 Al–2Li–2Cu–0.2Zr 合金夹杂物和力学性能的影响, 包括双级  $C_2Cl_6$  精炼工艺, 双级氩气旋转喷吹精炼工艺和双级复合精炼工艺。结果表明, 结合  $C_2Cl_6$  和氩气旋转喷吹的双级复合精炼工艺可以显著提高铸造 Al–2Li–2Cu–0.2Zr 合金的熔体纯净度和力学性能。与未精炼的合金相比, 通过双级复合精炼工艺得到的合金气孔缺陷和夹杂物的体积分数从 1.47% 下降到 0.12%, 固溶处理后合金的屈服强度、抗拉强度和伸长率分别从 113 MPa、179 MPa 和 3.9% 提高至 142 MPa、293 MPa 和 18.1%。合金熔炼过程中, 在加入锂之前首先使用  $C_2Cl_6$  精炼进行除气以及除掉熔体中较大尺寸的夹杂物, 在加入锂之后使用氩气旋转喷吹进一步除气以及除掉熔体中细小的悬浮夹杂物。双级复合精炼工艺不仅可以有效去除熔体中的气体和夹杂物, 还可以大幅度降低锂元素的氧化烧损, 结合两种精炼方法的各自优势, 取得显著的精炼效果。

**关键词:** Al–Li–Cu–Zr 合金; 精炼工艺; 显微组织; 熔体纯净度; 力学性能

(Edited by Xiang-qun LI)